

The surface eroding thermocouple for fast heat flux measurement in DIII-D

J. Ren,^{1,a)} D. Donovan,¹ J. Watkins,² H. Q. Wang,³ D. Rudakov,⁴ C. Murphy,⁵ A. McLean,⁶ C. Lasnier,⁶ E. Unterberg,⁷ D. Thomas,⁵ and R. Boivin⁵

¹University of Tennessee, Knoxville, Tennessee 37996-1410, USA

²Sandia National Laboratories, Livermore, California 94551, USA

³Oak Ridge Associated Universities, Oak Ridge, Tennessee 37830, USA

⁴University of California San Diego, San Diego, California 92093, USA

⁵General Atomics, San Diego, California 92186-5608, USA

⁶Lawrence Livermore National Laboratory, Livermore, California 94550, USA

⁷Oak Ridge National Laboratory, Oak Ridge, Tennessee 37830, USA

(Presented 18 April 2018; received 4 May 2018; accepted 15 June 2018;
published online 8 October 2018)

A novel type of surface eroding thermocouple (SETC) has been tested and demonstrated in the small angle slot (SAS) divertor of DIII-D for fast local heat flux measurements. The thermojunction of the SETC is formed between two thin (10 μm) ribbons, which are filed over to create microfiber junctions. These thermocouples are able to be exposed directly to the plasma at surface temperatures exceeding 2000 °C and are capable of sub-10 ms time resolution. Before installation in SAS, the SETCs were exposed in the lower DIII-D divertor during L-mode and H-mode discharges, from which results are presented. In preliminary tests, SETCs proved to be a qualified diagnostic to accurately measure both the intra-edge localized mode (ELM) and inter-ELM heat flux during H-mode shots with high frequency ELMs (hundreds of Hz) and to resolve heat flux profiles during strike point sweeps. The heat fluxes measured by using SETCs are consistent with the heat fluxes measured by using IR cameras and Langmuir probes. These new diagnostic capabilities will complement the existing IR camera measurements and will be of particularly significant value to measure surface heat flux in the SAS divertor or other regions where the IR camera lacks line of sight. *Published by AIP Publishing.* <https://doi.org/10.1063/1.5038677>

I. INTRODUCTION

The control of plasma facing surface heat fluxes is one of the key issues for magnetic fusion devices. When the heat and particle flux is above the damage limit and threshold for the plasma facing materials (PFMs), the life time of the first wall will reduce due to erosion, sputtering and cracking of its surface. In turn, the performance of core plasma is also largely determined by the exposure of its first wall components to energetic particles and radiation.¹ With future ITER demonstration and Demonstration Power Plant (DEMO) designs at even higher power densities, intensive power exhaust studies and heat load mitigation schemes have been demonstrated in existing magnetic fusion test devices.^{2,3} To provide valuable insight into the understanding of the physics of heat transport in the boundary plasma and forewarn the high surface temperature that may result in the erosion of plasma facing components, extensive and reliable diagnostics for heat flux measurements are essential.

Infrared (IR) cameras have been widely used in various fusion devices as a routine diagnostic due to their outstanding ability to obtain surface temperature and heat flux measurements.^{4,5} However, the field of view of IR cameras is not always sufficient to cover all the regions of interest in the divertor and is limited by the geometry of plasma facing components

(PFCs). So it is important to develop and implement new diagnostics for fast surface temperature and heat flux measurements in fusion devices, particularly in the divertor regions.

In order to address this crucial problem, we investigate a novel thermocouple designed for fast local temperature measurements named “Surface Eroding Thermocouple” (SETC). SETCs were first tested in the Alcator C-Mod Tokamak as part of the 2010 DOE Joint Research Target to characterize the heat flux footprint.⁶ In this project, an extensive system of thermal diagnostics—including Langmuir probes, SETCs, and calorimeters—was installed. During the cross-calibration, SETCs showed an excellent agreement in heat flux measurement with all other diagnostics. Moreover, the SETCs were also successfully used in studies of the divertor heat flux width and feedback control for divertor impurity seeding in C-Mod.^{7,8} Through systematic experiments, the SETCs proved to be a valuable surface heat flux diagnostic due to their fast time response and robust design allowing them to measure the surface temperatures under direct plasma exposure.

This work motivated implementing SETCs on many other fusion devices for fast local surface temperature and heat flux measurements. In this paper, the SETC diagnostic hardware and setup in DIII-D will be exhibited, and preliminary results will be shown.

II. HARDWARE AND SETUP

As shown in Fig. 1(a), a typical thermocouple consists of two dissimilar electrical conductors forming two junctions

Note: Paper published as part of the Proceedings of the 22nd Topical Conference on High-Temperature Plasma Diagnostics, San Diego, California, April 2018.

^{a)}rjun@utk.edu.

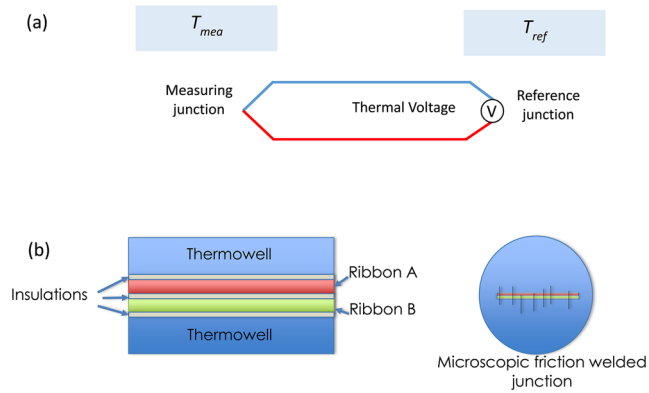


FIG. 1. Schematic diagram of (a) a traditional thermocouple and (b) a structure representation of a surface eroding thermocouple. Ribbons A and B are dissimilar materials that create a thermal voltage when joined.

at differing temperatures. The temperature-dependent voltage produced by using a thermocouple can be interpreted to measure temperature according to the Seebeck effect which can be written as

$$\nabla V = -S(T)\nabla T,$$

where ∇V is the voltage gradient between two junctions, (∇T) is the gradient in temperature, and $S(T)$ is a temperature dependent Seebeck coefficient. In practice, we use an ice-point (0°C) compensated circuit in the reference junction to determine the absolute temperature of the measuring junction.

The measuring junction in traditional thermocouples is so brittle that it is usually placed behind the sheath and tiles to protect from energetic particle flux. This results in a longer response time as the heat flux must propagate from the plasma facing surface to the thermocouple junction. SETCs are different from standard thermocouples in that the thermojunction is formed in a very thin layer at the surface of the sensor. As shown in Fig. 1(b), it is typically done by embedding two dissimilar metallic ribbons into a carrier body. These ribbons are electrically insulated from each other and the thermowell by sheets of thin ($5\ \mu\text{m}$) dielectric insulation (alumina or mica). Since the dielectric insulation between the two dissimilar ribbons is so thin, polishing the surface of the SETC creates metallic whiskers which bridge the dielectric and make hundreds of microscopic friction welded junctions, which are made parallel to one another. This kind of composite measuring junction is formed only on the very surface and leads to a fast thermal time response due to its direct plasma facing surface. In principle, any subsequent erosion of its surface will simply form new junctions while eroding the old junction. Hence, the SETC is not only a specialized diagnostic for characterizing the surface temperature evolution with a high

temporal resolution but also a robust diagnostic for long term use in a fusion device.

The SETC is commercially available from NANMAC Corporation. The original development work was completed in conjunction with NASA for rocket motor tests. Continued work at Nanmac, addressing newer materials and assembly methods to reduce cost and increase their reliability, has identified injection molding applications where high speed thermal measurements and robustness help to achieve 10%–20% operating cost reductions.⁹ In the design of SETCs for DIII-D, a pair of $50\ \mu\text{m}$ thick and 3 mm wide ribbons made of type C thermocouple conductors (W-5% Re and W-26% Re) was sandwiched between alumina dielectric insulator layers and surrounded by a Mo pin thermowell [shown in Fig. 2(a)]. The type C junction was chosen because of its large measurement range (0 – 2320°C), minimal erosion, and compatibility with common PFC materials. In order to test SETCs before the permanent installation, exposures were performed using the Divertor Material Evaluation System (DiMES) in DIII-D.¹⁰ As shown in Fig. 2(b), two SETCs installed in a customized ATJ graphite sample were exposed in DiMES in two different radial locations during both L-mode and H-mode plasma discharges with the outer strike point on the lower divertor shelf. During these shots, SETCs were fixed at near scrape-off layer (SOL) or were swept across by the outer strike point (OSP). Before the exposure, an oxide layer caused by high temperature baking covered the surface of the SETCs. The surface of SETCs appears bright after exposure to the plasma, due to cleaning of the exposed surfaces by energetic particles and heat flux from the SOL plasma. No visible melting or erosion was observed on the surface of SETCs. During the SETC testing experiment, plasma had a good performance, and no obvious effective Z or Mo line emission increase was found.

Data acquisition for the SETC diagnostic in DiMES was accomplished using a Dewetron DS-NET system with 10 kHz sampling rate per channel, built-in cold junction compensation, 24 bit resolution, and 1200 V galvanic channel-to-channel and channel-to-chassis isolation. Signals from the SETCs to the acquisition system are transported by normal copper leads.

III. DATA PROCESSING AND INTERPRETATION

Since the SETC response is influenced by time-varying magnetic fields, care must be taken in the analysis to account for this. Figure 3(a) shows the original temperature signal acquired by using the SETC in a typical H-mode plasma shot. A significant magnetic pickup appeared in the temperature signal when the B-coil current rose rapidly before the plasma shot and decayed for a long time after the shot. By assuming a linear coefficient (γ) between the rate of B-coil change

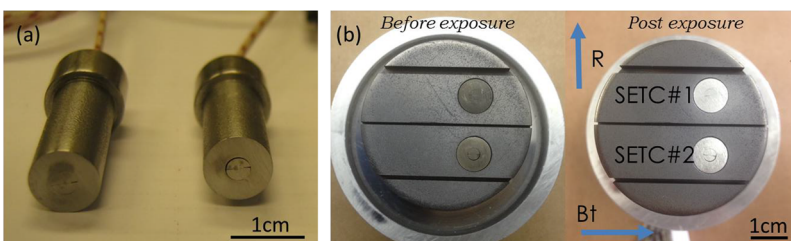


FIG. 2. (a) Photo of surface eroding thermocouples with molybdenum body and (b) DiMES sample showing the two thermocouples before and after exposure.

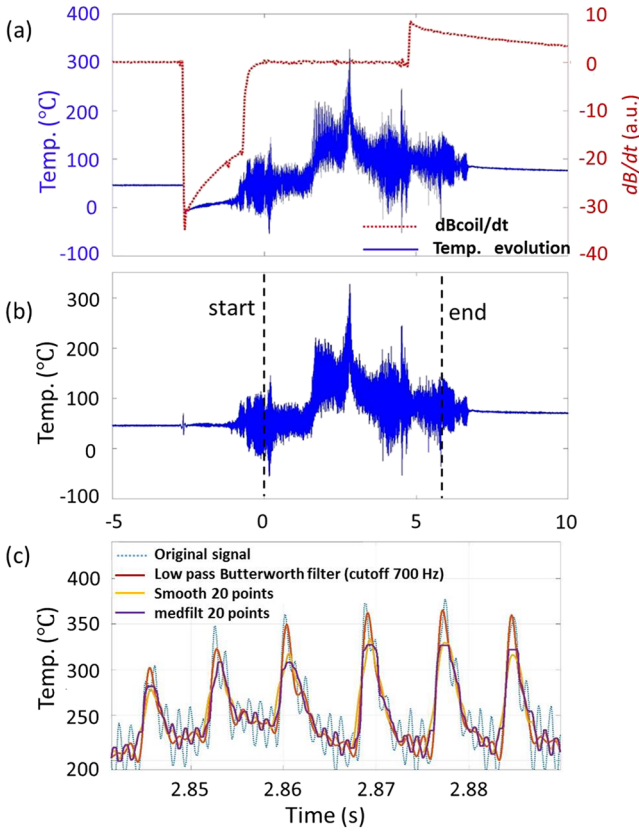


FIG. 3. (a) Evolution of original temperature measured by using the SETC and the rate of B-coil current change, (b) temperature signal after the pickup was removed, and (c) a comparison of filtering effect among several software filters.

(dB/dt) and the pickup in the temperature signal, the pickup can be eliminated by simply removing $\gamma(dB/dt)$ from the original temperature signal [shown in Fig. 3(b)].¹¹ Several software filters, including an averaging filter, median filter, and low pass Butterworth filter, were implemented to reduce noise on the SETC signal after the magnetic pickup was removed. As shown in Fig. 3(c), the low pass Butterworth filter with 700 Hz cutoff frequency showed the best filtering effect with the minimum distortion in wave shape.

After removing the pickup and minimizing the noise from the temperature signal measured by using the SETC, the heat flux impinging on the surface of the SETC is calculated by using a two dimensional finite difference thermal model compiled by MATLAB.¹² If we consider the SETC as a structure assembled by finite elements with no internal heat source, the inflow of heat flux from one element will equal the sum of outflows of heat flux of this element and the increase in internal energy. For the element $T_{2,2}$ shown in Fig. 4, its temperature at the next moment in time ($T_{2,2}^{t+1}$) can be expressed as

$$T_{2,2}^{t+1} = T_{2,2}^t + \Delta\tau \times Q_{total}^t / \rho\omega^3 C_p,$$

where $T_{2,2}^t$ is the temperature at present, $\Delta\tau$ is the time interval between those two moments (which is the sampling time of the SETCs), ρ and C_p are the temperature-independent density and specific heat capacity, respectively, and ω is the length of each side of the element. Q_{total}^t represents the absolute value of inflowing heat flux of this element, which can be quantified as

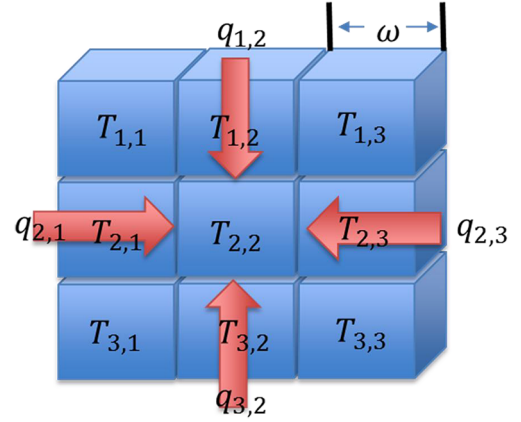


FIG. 4. Schematic diagram of thermal modeling.

$$\begin{aligned} Q_{total}^t &= Q_{1,2}^t + Q_{2,1}^t + Q_{2,3}^t + Q_{3,2}^t \\ &= -\lambda\omega \left((T_{2,2}^t - T_{1,2}^t) + (T_{2,2}^t - T_{2,1}^t) + (T_{2,2}^t - T_{2,3}^t) \right. \\ &\quad \left. + (T_{2,2}^t - T_{3,2}^t) \right), \end{aligned}$$

where λ is the temperature-independent heat conductivity of the SETC material and $T_{m,n}^t$ is the temperature of the corresponding element at the present time.

Before each plasma shot, the whole SETC structure was assumed to achieve thermal equilibrium with the surrounding PFC material, due to the more than 10 min intervals between shots in DIII-D allowing time for temperatures to equilibrate. The temperature was measured by using the SETC before the shot was given as the initial condition of the modeling. However, the temperatures measured by using the SETCs during the shot are unable to be given as boundary conditions of the modeling because the thermal contact between the measurement junction and the bulk of the SETC is not considered to be a perfectly joined solid mass. An assumption regarding the surface heat transmission coefficient (α) must be defined here as

$$q_{bulk} = q_{sur} = \alpha \times (T_{sur} - T_{bulk}),$$

where q_{sur} is the heat flux from the SOL plasma impinging on the surface junction, q_{bulk} is the heat flux coming from the surface junction into the SETC bulk, and T_{sur} and T_{bulk} are the temperatures of the surface junction and SETC bulk, respectively. Assuming that the measuring junction is so small that its specific heat capacity is zero, the q_{bulk} will be equal to q_{sur} . The surface heat transmission coefficient (α) is a factor to quantify the ability of heat to transfer from the junction surface to the SETC bulk.¹³

How to quantify α is very important in the calculation of heat flux. One method to quantify α for a given SETC is to use the law of conservation of energy. As shown in Fig. 5, total deposited energy on the SETC surface in a typical shot is calculated by integrating the heat flux in time using different values of α from 2 kW/m² K to 100 kW/m² K. Since there is no heat flux impinging on the surface of the SETCs after the plasma shot, the deposited energy curve should be flat. From this approach, it appears that 20 kW/m² K is an appropriate value for the surface heat transmission coefficient in this shot. This α will be used in thermal modeling to calculate perpendicular heat flux on the PFC structure of the SETC.

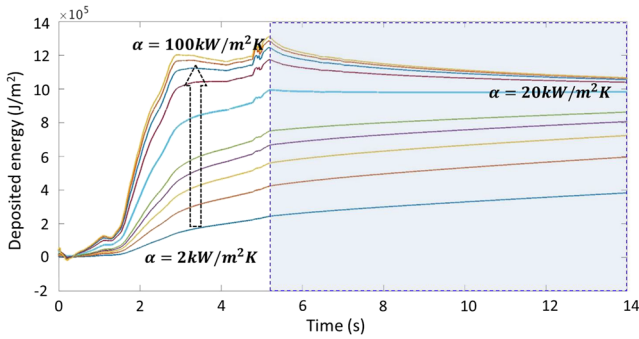


FIG. 5. Total deposited energy on the SETC calculated by integrating the heat flux using different α .

IV. PRELIMINARY RESULTS

As shown in part II, two SETCs were exposed on the lower divertor shelf at radii of 1.4785 m and 1.4947 m, respectively. Sweeps of the outer strike point were performed from inboard of DiMES (1.425 m) to outboard of DiMES (1.655 m) in both L-mode and H-mode plasma, allowing us to study the SETC response to the strike point sweeps and bursts of Edge Localized Modes (ELMs). The evolution of the measured temperature profile in one H-mode plasma shot with 3.5 MW auxiliary Electron Cyclotron Heating (ECH) and $5 \times 10^{13} \text{ cm}^{-3}$ main plasma density is shown in Fig. 6. As expected, the temperature on the SETC decreased as the OSP moved away from the SETC and increased as the OSP moved toward the SETC. The maximum temperature of the SETC occurred when the outer strike point was located about 2 mm inboard of the SETC junction. The temperature decayed quickly after the outer strike point swept over the SETC, placing the SETC in the private flux region where there is drastically lower heat flux, which means that the SETCs provide a sufficiently fast surface temperature measurement to resolve heat flux profiles during strike point sweeps. In addition, it was noted that all the spikes in temperature measured by using the SETC perfectly kept pace with the $D\alpha$ emission, which is usually used

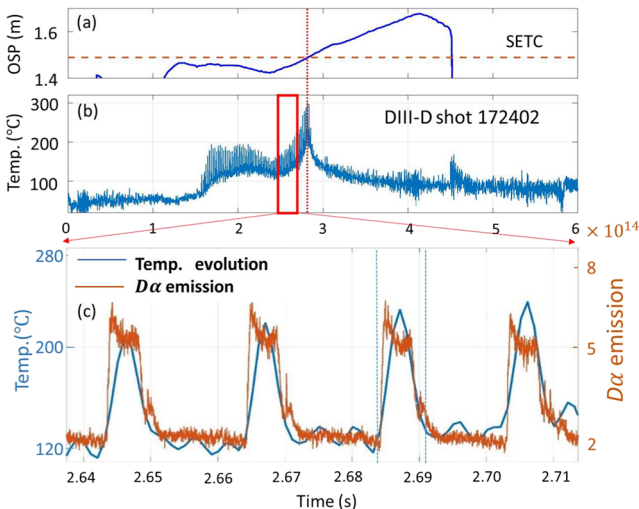


FIG. 6. (a) The time evolution of the outer strike point position, (b) temperature measured by using the SETC in DiMES, and (c) a plot comparing temperature and $D\alpha$ emission on a time scale where ELMs can be resolved.

to characterize ELMs. This implies that the SETC is able to respond to the heat flux during the ELMs.

The extensive diagnostics on the lower divertor of DIII-D provided an excellent opportunity to perform a cross-calibration of the SETC with the IR camera and equation for heat flux from the Langmuir probes. As shown in Fig. 7(a), the heat fluxes measured by using the SETC had good consistency with the heat fluxes measured by using IR camera and Langmuir probes in an L-mode plasma shot with the OSP sweeping across the DiMES from the inboard side to the outboard side. The Langmuir probe providing heat flux data in this plot was close to the SETC in the outboard side. In H-mode plasma, a comparison of the measured heat flux between the SETC and IR camera is shown in Fig. 7(b). We can see that the base line of heat flux measured by using the SETC had a good agreement with the base line of heat flux provided by the IR camera during inter-ELMs. It was also noted the magnitude of intra-ELM heat flux measured by using the SETC was consistent with what was measured by using the IR camera. Moreover, the spike in heat flux measured by using the SETC did not appear when the SETC was located in the private flux region but rather only occurred when the SETC was in the SOL. This gives us greater confidence that the SETCs can be considered a qualified diagnostic to accurately measure both

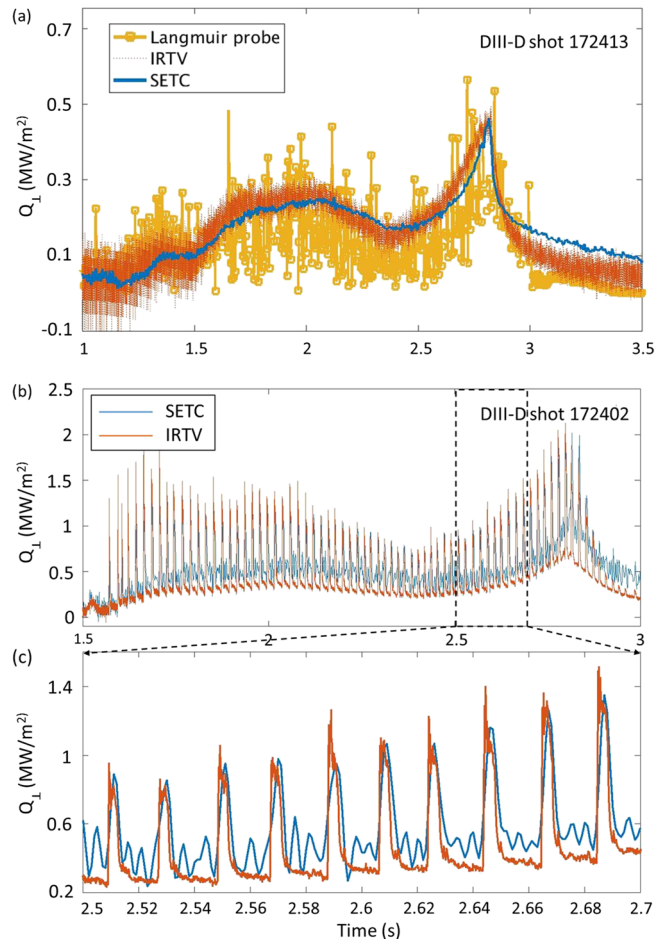


FIG. 7. (a) A comparison of the measured heat flux between the SETC, Langmuir probe, and IR camera in L-mode and [(b) and (c)] a comparison of the measured heat flux between the SETC and IR camera in ELMing H-mode.

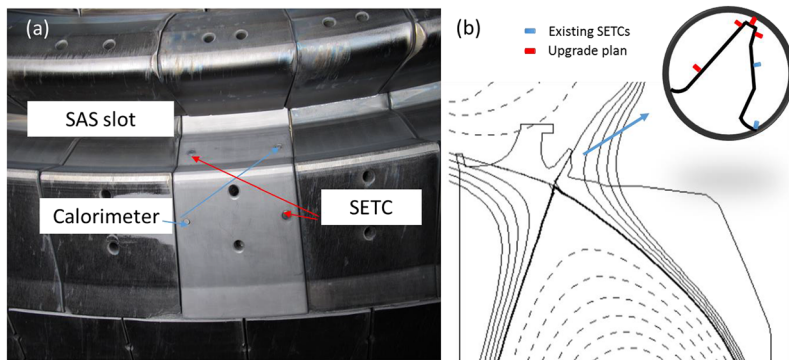


FIG. 8. (a) Photo of the SAS tile after SETCs were installed and (b) existing SETCs and an upgrade plan shown in a sketch of the SAS divertor on the DIII-D tokamak.

the intra-ELM and inter-ELM heat flux during H-mode shots in DIII-D.

V. FUTURE WORK IN DIII-D DIVERTOR

In DIII-D, a closed divertor concept called the small angle slot (SAS) divertor has been designed and implemented to enhance the buildup of neutral density in a localized region near the plasma strike point. Spreading of the cooling front across the divertor target, with the slot gradually flaring out from the strike point, has been predicted by SOLPS modeling and investigated experimentally. The most critical feature of the SAS divertor is manifested by its small angle at the outboard side end of the divertor slot (shown in Fig. 8). In this small slot, Langmuir probes were the only diagnostics to provide heat flux information on the divertor target. But the Langmuir probes have limitations because the precision of the heat fluxes measured by using Langmuir probes is largely dependent on the definition of the sheath heat flux transmission coefficient, a fundamental physical quantity whose theoretical value is ~ 7 , but has varied from 2 to 20 in experimental measurements.^{14,15} In this case, developing the SETCs, which can provide fast and accurate heat flux measurements at the target plate, may help understand the performance of this divertor concept.

Two SETCs were installed into a tile of the SAS divertor at toroidal 220° [shown in Fig. 8(a)]. Adapting for long term routine employment, a 32 channel, 10 kHz sampling rate D-tAcq data acquisition system has been set up for SETCs in the SAS divertor. Signals from the SETCs to the digitizer were transported through an isolated amplifier, RC filter, and fiber optic link to avoid the machine potential leaving the device and to reduce noise. These SETCs are providing valuable surface temperature and heat flux data in the SAS divertor in a location where the IR cameras have limited lines of sight.

For future work in DIII-D, an upgraded set of SETCs are planned to be implemented in the SAS divertor during the coming long term vent in 2018. More SETCs will be installed in the SAS divertor to create a poloidal array [shown in Fig. 8(b)], which will be able to provide an accurate and high temporal resolution temperature and heat flux distribution profile. A new compact SETC design based on insulation coating is being developed for minimizing the size of SETC. It will simplify the installation and increase the spatial resolution of SETC. In addition, an optimized and customized thermocouple feedthrough and a twisted pair or coaxial thermocouple cable

will be developed to reduce the noise and magnetic pickup. All this will be very useful to improve the diagnostic capabilities of the closed divertor experiments and contribute to studying the physics of heat transport in the SAS divertor.

ACKNOWLEDGMENTS

The authors would like to express their gratitude to Dr. T. Gray (Oak Ridge National Laboratory) and D. Brunner (Massachusetts Institute of Technology) for their support. They also acknowledge the technical support by Mr. H. Dwyer and D. Kuszpa at NANMAC. This work was supported by the U.S. Department of Energy under Contract Nos. DE-SC0016318, DE-FC02-04ER54698, DE-AC05-00OR22725, DE-FG02-07ER54917, DE-NA0003525, and DE-AC52-07NA27344.

This report was prepared as an account of work sponsored by an agency of the United States Government. Neither the United States Government nor any agency thereof, nor any of their employees, makes any warranty, express or implied, or assumes any legal liability or responsibility for the accuracy, completeness, or usefulness of any information, apparatus, product, or process disclosed, or represents that its use would not infringe privately owned rights. Reference herein to any specific commercial product, process, or service by trade name, trademark, manufacturer, or otherwise, does not necessarily constitute or imply its endorsement, recommendation, or favoring by the United States Government or any agency thereof. The views and opinions of authors expressed herein do not necessarily state or reflect those of the United States Government or any agency thereof.

- ¹A. W. Leonard, *Plasma Phys. Controlled Fusion* **60**(4), 044001 (2018).
- ²K. Tobita *et al.*, *Nucl. Fusion* **47**(8), 892 (2007).
- ³M. A. Makowski *et al.*, *Phys. Plasmas* **19**(5), 056122 (2012).
- ⁴D. N. Hill *et al.*, *Nucl. Fusion* **28**(5), 902 (1988).
- ⁵C. J. Lasnier *et al.*, *Fusion Sci. Technol.* **53**(2), 640–666 (2008).
- ⁶D. Brunner *et al.*, *Rev. Sci. Instrum.* **83**(3), 033501 (2012).
- ⁷D. Brunner *et al.*, *Rev. Sci. Instrum.* **87**(2), 023504 (2016).
- ⁸D. Brunner *et al.*, *Nucl. Fusion* **57**(8), 086030 (2017).
- ⁹J. Nanigian, paper presented at the Defense and Security Symposium, 2006.
- ¹⁰D. L. Rudakov *et al.*, *Phys. Scr.* **T138**, 014007 (2009).
- ¹¹J. G. Watkins *et al.*, *Rev. Sci. Instrum.* **74**(3), 1574–1577 (2003).
- ¹²A. J. Ghajar and Y. A. Cengel, *Details About Heat and Mass Transfer: Fundamentals and Applications* (McGraw-Hill Education, 2014).
- ¹³T. Eich *et al.*, *Plasma Phys. Controlled Fusion* **47**(6), 815 (2005).
- ¹⁴D. Donovan *et al.*, *J. Nucl. Mater.* **438**, S467–S471 (2013).
- ¹⁵J. G. Watkins *et al.*, *J. Nucl. Mater.* **463**, 436–439 (2015).